Mathematics and Computer Science
2022; 7(6): 106-112
http://www.sciencepublishinggroup.com/j/mcs
doi: 10.11648/j.mcs.20220706.11
ISSN: 2575-6036 (Print); ISSN: 2575-6028 (Online)

Mobile Robot Positioning System of Adaptive Unscented Kalman Filter with Forgetting Factor

Wenliang Zhu[1], Junjie Huang[2, *], Yunpeng Zhou[1], Chengxiao Zhu[3]

[1]School of Mechanical Engineering, Jiangsu Ocean University, Lianyungang, China

[2]School of Ocean Engineering, Jiangsu Ocean University, Lianyungang, China

[3]School of Advanced Technology, Xi'an Jiaotong-liverpool University, Suzhou, China

Email address:

525954636@qq.com (Junjie Huang)

[*]Corresponding author

To cite this article:

Wenliang Zhu, Junjie Huang, Yunpeng Zhou, Chengxiao Zhu. Mobile Robot Positioning System of Adaptive Unscented Kalman Filter with Forgetting Factor. *Mathematics and Computer Science*. Vol. 7, No. 6, 2022, pp. 106-112. doi: 10.11648/j.mcs.20220706.11

Received: November 6, 2022; **Accepted**: November 21, 2022; **Published**: November 30, 2022

Abstract: For the problem of inaccurate positioning of mobile robots in complex industrial environments, a multi-sensor combination localization method for omnidirectional mobile robots is proposed that incorporates the unscented Kalman filter (UKF), Real-Time Kinematic (RTK), and Inertial Measurement Unit (IMU). Firstly, the position information of the mobile robot is obtained by Real-Time Kinematic (RTK) and Wheel Odometry respectively. Secondly, the inertial measurement unit (IMU) determines the cart yaw angle while dual RTK is proposed to solve the yaw angle in real-time. Finally, the position and yaw angle data are input to the unscented Kalman filter in real time. This paper proposes the F-AUKF algorithm, which optimizes the traditional unscented Kalman filter algorithm by introducing a forgetting factor in order to improve the robustness of mobile robot localization for continuous operation in complex industrial building environments. The experimental results show that the F-AUKF algorithm eventually achieves a positioning accuracy about 10 times higher than that of a single odometer, about 6 times higher than that of a single RTK and about 3 times higher than that of the traditional UKF algorithm, effectively improving the problem of dispersion of the filtering effect after a long period of operation and providing better stability.

Keywords: Outdoor Mobile Robots, Multi-sensor Fusion Positioning, F-AUKF, Forgetting Factor

1. Introduction

High-precision positioning is one of the key technologies for mobile robots since position and orientation are the main demands of mobile robot navigation, guidance, and steering control. Dead reckoning of location and orientation by making use of kinematic model and shaft encoder as means of incremental measuring is commonly used in indoor applications of mobile robots. However, in outdoor environment, mobile robots must traverse in uneven and soft earth terrains, the localization error of dead reckoning will be rapidly accumulated due to the slipping movement and other flaws of wheels and result in a relatively low accuracy. The INS/GNSS (Initial Navigation System/Global Navigation Satellite System) multiple sensor fusing localization technology has been proven to be an effective method [1-5]. The short-term accuracy of INS combined with the long-term accuracy of GNSS compensate for the drawbacks of a single sensor. Although a large body of research has been published on multi-sensor fusion positioning problems, most of the research applies simulations to verify the effectiveness of the algorithms. In practical applications, more factors need to be taken into consideration. For example, to compensate the defects of a single sensor in order to improve localizing accuracy of the mobile robot so as to promote the accuracy of trajectory tracking. Furthermore, the robustness of the control method needs to be improved as factors such as the unknown environment and the uncertainty of disturbances can have an impact on the actual effectiveness of the control method. This paper focuses on situations where the RTK signal is weak due to complex industrial environments (e.g., building blockage) or weather factors (e.g., thick cloud cover).

Fu Jun et al [1] propose a new adaptive UKF algorithm to improve UWB indoor positioning accuracy by constructing a state error compensation function and correcting the state deviation in real-time. Hu Fengjun et al [6] propose a multi-sensor fusion positioning correction algorithm based on EKF with adaptive error and refine the covariance using the evolutionary iteration mechanism of the genetic algorithm is verified by experimental simulation. Din Menatalla-Shehab-El et al [7] apply the improved UKF in SOC power estimation and use adaptive covariance least squares to calculate the measurement noise covariance, which improves the accuracy of estimation. Juqiang Feng et al [8] introduce the forgetting factor into the unscented Kalman filtering, which eliminates the problem that the traditional UKF method is greatly affected by system noise and observation noise with high accuracy, great convergence and robustness in battery SOC estimation. This article improves the accuracy of localization and orientation of the mobile robot by adopting the integrated method of fusing RTK localization data, odometer data and inertial measurement unit data, and introduces the adaptive unscented Kalman filtering algorithm with forgetting factor in order to improve the robustness of the mobile robot tracking control system under the long-time operation. Finally, a mobile robot control experiment is designed on an omni-directional self-guided mobile robot with Mecanum wheels. The experiment validates the effectiveness and advantages of the algorithm in the control experiment.

2. RTK- Real-Time Kinematic Difference Positioning Method

The essential operational principle of RTK is based on the fact that the GNSS systematic error varies slowly and has time-spatial associations. Calculating the differences between two receivers can eliminate most of the errors to improve the positioning accuracy. As shown in Figure 1, the basic differential positioning system consists of three components: the reference station, the onboard RTK (mobile station) and the data exchange (mutual communication between the two stations). The correction data received from base station shall be positioning differences, pseudo range differences and carrier-wave phase differences [9]. This paper adopts the carrier-wave phase difference algorithm for the RTK. The kernel of the algorithm is to calculate the pseudo ranges of multiple satellites both between on board station and assistant base station by suppressing errors resulting from the influences of atmosphere disturbance, relativity error, clocking error and other causes to increase the accuracy. The pseudo-range is the biased distance between satellites and the stations, which is calculated by measuring the transmission time of the signals transmitted by every single satellite [10, 11].

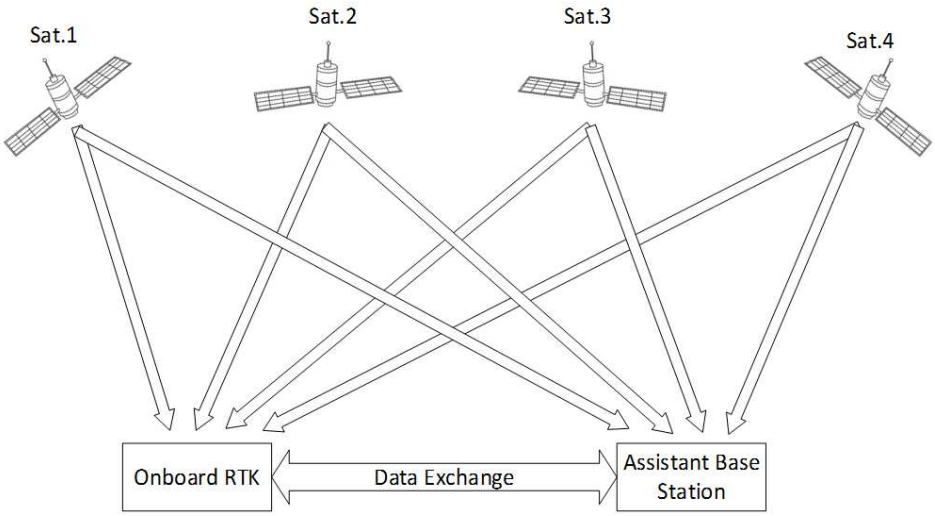

Figure 1. *Differential Positioning Basis.*

When GPS positions were first obtained, they were represented in the Earth-centered, Earth-fixed coordinate system (ECEF), that is the World Geodetic Coordinate System defined in 1984 (WGS 84). It is necessary to transform coordinates of ECEF into local frame. The problem arises that if any point used in the positioning has incorrect local coordinates (determined by conventional surveying methods in general) or incorrect WGS 84 coordinates owing to GPS flaws, the estimated transformation parameters will be incorrect and all the RTK measurements using the positioning will be influenced.

Figure 2 illustrates a RTK system consists of an omni-directional self-guided mobile robot platform mounted with 2 RTK devices, an IMU device and a stationary RTK station in the open space outside the factory. The straight line connects the RTK devices passes through the geometrical center for the robot and is perpendicular to the x-axis of the robot. The IMU is installed at the geometrical center of the robot. Two RTK receivers are installed on the cart and their connection lines are perpendicular to the motion axis. The benefit of installing RTKs in perpendicular to the motion axis is that the yaw angle measured by dual RTKs is the one of the robot's

motions without transform.

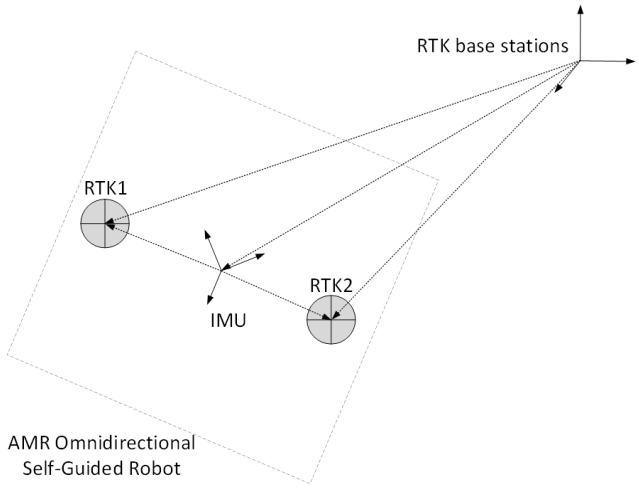

Figure 2. *A demonstration of two mobile RTK stations and a RTK base station.*

The yaw angle of the robot's motion θ_{RTK} is represented as:

$$\theta_{RTK} = \arctan2\big((y2 - y1), (x2 - x1)\big) \quad (1)$$

Where $(y2 - y1)$ and $(x2 - x1)$ are obtained from the positions of the two antennas in the tangent plane of local the surface. See Figure 3.

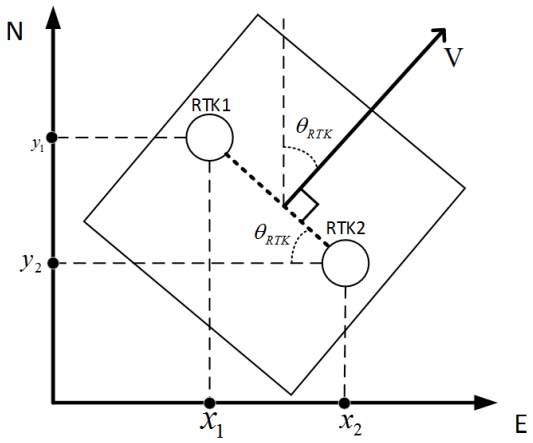

Figure 3. *Determining the yaw angle using dual RTK.*

Figure 4. *Diagram of the actual RTK installation.*

3. The Multi-sensor Fusion Filtering Algorithm

3.1. Fusion Positioning Framework

The algorithm applying the unscented Kalman Filter (UKF) to the fusion of the wheel odometer sensor, inertial measurement unit (IMU) sensor and Real-time Kinematic (RTK) sensor devices. The positioning information provided by the sensors are used in estimations of the location and yaw angle of the robot. In general, UKF consists of two parts: the prediction step and the update step. The prediction step uses positioning information from the wheel odometry (X_{Odom}, Y_{Odom}) . The update step uses IMU posture information θ_{IMU} and positioning information provided by RTKs $(X_{RTK}, Y_{RTK}, \theta_{RTK})$as its observation.

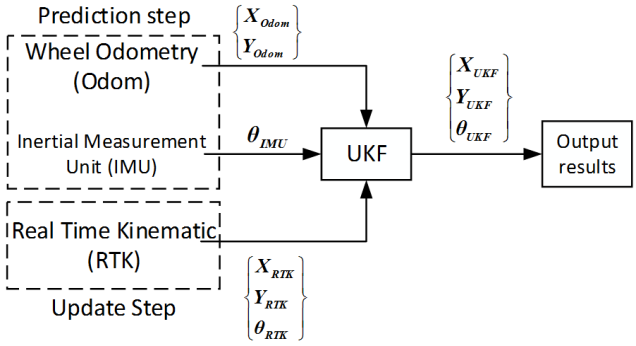

Figure 5. *Block diagram of the fusion positioning process.*

The present researches on using the Kalman filter in the multi-sensor fusion navigation can be divided into two classes with the state of the estimation system: the methods of direct and indirect approximations. Both deploy the advantages of the fast regression fusing algorithm to administrate the lots of row sensor data in navigation devices. The indirect methods take the navigation errors of the subsystems INS and GNSS as the system state and calculate their optimal estimates. The direct method takes the output navigation parameters of the subsystem as the system state and deduces the navigation solution of the integrated system directly by Kalman filtering. Compared to the indirect method, the direct method has the following advantages: (I) system state equation directly describes the dynamic process of the resolving of the navigation parameters which reflects the real variations of the states in precision. It is more accurate than the first-order approximation provided by the indirect method. (II) The dynamic calibration equation of INS is the essential part of the system state equation, the Kalman filter not only obtains the navigation solution of the dynamic calibration equation but also plays a critical role in filter estimation, avoiding a great number of repeated calculations. However, applying the direct method to INS/GNSS integrated navigation introduces nonlinearities into the system equation, traditional linear Kalman Filter (KF) is not suitable to handle the nonlinearities involved. The Extended Kalman

Filter (EKF) is a common algorithm used for nonlinear system state estimation. It is an approximation method where the nonlinear system is linearized by Taylor series so that the linear KF can be applied. The Unscented Karlman Filter (UKF) is considered an improvement of EKF, they both share the same basis, the main differences are the representation of the Gauss random variable in the equations. The UKF uses a finite number of Sigma points as information about the system's state change and estimation capability to obtain another changing state focus. Then the mean and covariance of the changed focus are used to obtain the state estimate and the state estimate error covariance, which avoids the complex evaluation of Jacobian matrix and makes the algorithm easier to implement [12-15].

Suppose the working environment for the omnidirectional mobile robot is an ideal horizontal two-dimensional environment. Establish the coordinate frame in the plane where the omnidirectional mobile trolley is located, with east as the x-axis positive direction and north as the y-axis positive direction. The coordinates of the robot's position and speeds in this frame are the state vector. Given the process and measurement noises have Gaussian distribution of 0 mean, The discrete system state equation can be described as follow:

$$\begin{cases} X_k = F_{k-1}X_{k-1} + W_k \\ Z_k = H_k X_k + V_k \\ W_k \sim (0, Q_k) \\ V_k \sim (0, R_k) \end{cases} \tag{2}$$

X_k is the discrete state equation at time k, Z_k is the measurement equation, F_{k-1} is the state transfer matrix, H_k is the measurement transfer matrix. W_k and V_k are the process and measurement noises of 0 mean. Q_k and R_k are covariant matrix of W_k and V_k respectively.

The UKF can be divided into 4 steps: initialization, unscented transform (UT), time updating and measurement updating.

(1) Initialization.

$$\begin{cases} \hat{X}_0 = E[X_0] \\ P_0 = E[(X_0 - \hat{X}_0)(X_0 - \hat{X}_0)^T] \end{cases} \tag{3}$$

where $\hat{X}_0$ is the initialized state estimation vector and P_0 is the initialized error covariance matrix.

(2) UT transfer. In this step, some samples are selected out of the original samples set under certain selecting rule so the sub-set selected samples shall have the same mean and variance as the original set. Then the selected samples shall be applied into the nonlinear system functions and corresponding range of the nonlinear functions shall be available to calculate the mean and variance transferred.

1) computing 2n+1 Sigma point (sample), n stands for the number of dimensions of the state space, In the system under scrutiny, it shall be,

$$\begin{cases} \xi_{k-1}^0 = \hat{X}_{k-1}, i = 0 \\ \xi_{k-1}^i = \hat{X}_{k-1} + \left(\sqrt{(n+\delta)P_{k-1}}\right)_i, i = 1,2,\cdots,n \\ \xi_{k-1}^i = \hat{X}_{k-1} + \left(\sqrt{(n+\delta)P_{k-1}}\right)_i, i = n+1,\cdots,2n \end{cases} \tag{4}$$

In the formula $\left(\sqrt{P_{k-1}}\right)_i$ represents the the i-th row of the matrix's square root; δ is the ratio factor, such that $\delta = \alpha^2(n+k) - n$ in it, α is an adjustment parameter that determines the distribution of Sigma points around $\hat{X}_{k-1}$, which is usually set to a small positive value. And α is taken to be 0.0001 in this paper.

2) determining the weight of the Sigma points.

$$\begin{cases} \omega_a^0 = \frac{\delta}{n+\delta} \\ \omega_c^0 = \frac{\delta}{n+\delta} + 1 - \alpha + \beta \\ \omega_a^i = \omega_c^i = \frac{\delta}{2(n+\delta)}, i = 1,2,\cdots,2n \end{cases} \tag{5}$$

where ω of subscript a is the mean and with subscript c is the covariance, and superscript is the index of Sigma points. β is the state distribution parameter whose value can adjust the accuracy of the variance. And β is taken as 2 in this paper.

(3) Time update. The Sigma point set $\boldsymbol{\xi}_{k-1}^i$ is used as the state vector of UKF. The system state equation is used to find the next predicted state value $\xi_{k|k-1}^i$ of the system. The predicted mean $\hat{X}_{k|k-1}$ and variance $P_{k|k-1}$ are calculated.

$$\begin{cases} \xi_{k|k-1}^i = F * \xi_{k-1}^i + W_i, i = 0,1,2,\cdots,2n \\ \hat{X}_{k|k-1} = \sum_{i=0}^{2n} \omega_a^i \, \xi_{k|k-1}^i \\ P_{k|k-1} = \sum_{i=0}^{2n} \omega_a^i \, (\xi_{k|k-1}^i - \hat{X}_{k|k-1})(\xi_{k|k-1}^i - \hat{X}_{k|k-1})^T + Q_k \end{cases} \tag{6}$$

(4) Measurement update. Applying estimated states $\xi_{k|k-1}^i$ to the measurement equation. Estimated observation values $Z_{k|k-1}^i$ are computed, by computed the weighed summary to obtain the estimated system means $\hat{Z}_{k|k-1}$ and covariance $P_{Z_k Z_k}$.

$$\begin{cases} Z_{k|k-1}^i = H_k \xi_{k|k-1}^i + V_i, i = 0,1,\cdots,2n \\ \hat{Z}_{k|k-1} = \sum_{i=0}^{2n} \omega_a^i Z_{k|k-1}^i \\ P_{Z_k Z_k} = \sum_{i=0}^{2n} \omega_c^i \, (Z_{k|k-1}^i - \hat{Z}_{k|k-1})(Z_{k|k-1}^i - \hat{Z}_{k|k-1})^T + R_k \end{cases} \tag{7}$$

Computing $P_{X_k Z_k}$ of the state prediction and observation estimation.

$$P_{X_k Z_k} = \sum_{i=0}^{2n} \omega_c^i \left[\left(\xi_{k|k-1}^i - \hat{X}_{k|k-1}\right)\left(Z_{k|k-1}^i - \hat{Z}_{k|k-1}\right)^T \right] \tag{8}$$

Computing the gain of Kalman filter K_{k+1}.

$$K_{k+1} = P_{X_k Z_k} * P_{Z_k Z_k}^{-1} \tag{9}$$

Finally, computing the state update $\hat{X}_k$ and covariance update P_k of the system.

$$\hat{X}_k = \hat{X}_{k|k-1} + K_{k+1}(Z_k - \hat{Z}_{k|k-1}) \quad (10)$$

$$P_k = P_{k|k-1} - K_{k+1}P_{X_kZ_k}^T \quad (11)$$

3.2. The Improvement of Self-adaptive UFK Algorithm by Adding Forgetting Factor (F-AUKF)

The UKF is obviously advantageous over traditional KF and EKF. However, the process noise covariance matrix of the errors and the signal measurement noise covariance matrix can cause the filtering effect to diverge after a longer period of filtering. Meanwhile, the accuracy of the UKF algorithm is influenced by the initial value of the process significantly. If the initial state equation and variance errors are relatively large, it will affect the state mean and the estimated value. This paper proposes the F-AUKF algorithm, the variance inflation principle is used to reduce the influence of the initial state error on the filtering process. In other words, the system noise covariance is self-adaptively inflated with the measurement noise covariance matrix to adjust their effects in the filtering process.

Forgetting factor b is introduce in this paper so as to avoid the divergence and to improve the accuracy of the algorithm.

Updating the covariance of system noise $\hat{Q}_k$ and the measurement noise covariance $\hat{R}_k$:

$$\begin{cases} \hat{Q}_k = (1-d_{k-1})\hat{Q}_{k-1} + \\ \quad d_{k-1}(K_{k+1}e_k e_k^T K_{k+1}^T + P_k - P_{k|k-1}) \\ \hat{R}_k = (1-d_{k-1})\hat{R}_{k-1} + d_{k-1}(e_k e_k^T - P_{Z_kZ_k}) \\ e_k = Z_k - \hat{Z}_{k|k-1} \\ d_k = (1-b)(1-b^{k+1})^{-1}, b \in [0,1] \end{cases} \quad (12)$$

Where e_k is the residual, d_k is the self-adaptive factor and b is the forgetting factor.

The forgetting factor b has a value between 0.95 and 1 generally, it is 0.98 in this paper. In order to improve the robustness of the system, a self-adaptive factor d_k is used in this paper to prevent the filtering effect of UKF from being too sensitive to the value of the forgetting factor b.

4. The Experimental Analysis

In order to verify the accuracy improving effectiveness of the F-AUKF algorithm compared to the traditional UKF, the experiments are carried out in open and almost flat outdoor field with the robot (the altitude can be omitted). The RTK and odometer share the same coordinate system in order to facilitate the comparison. Figure 5 shows the actual experimental field.

Figure 6. *QT-based development of the upper computer.*

The vehicle movement (CM for circular motion mode, LM for linear motion mode) can be controlled using the self-developed QT upper computer. The green dashed line is the theoretical trajectory and the blue solid line is the actual trajectory, which can reflect the real-time latitude, longitude and real-time coordinates of the vehicle.

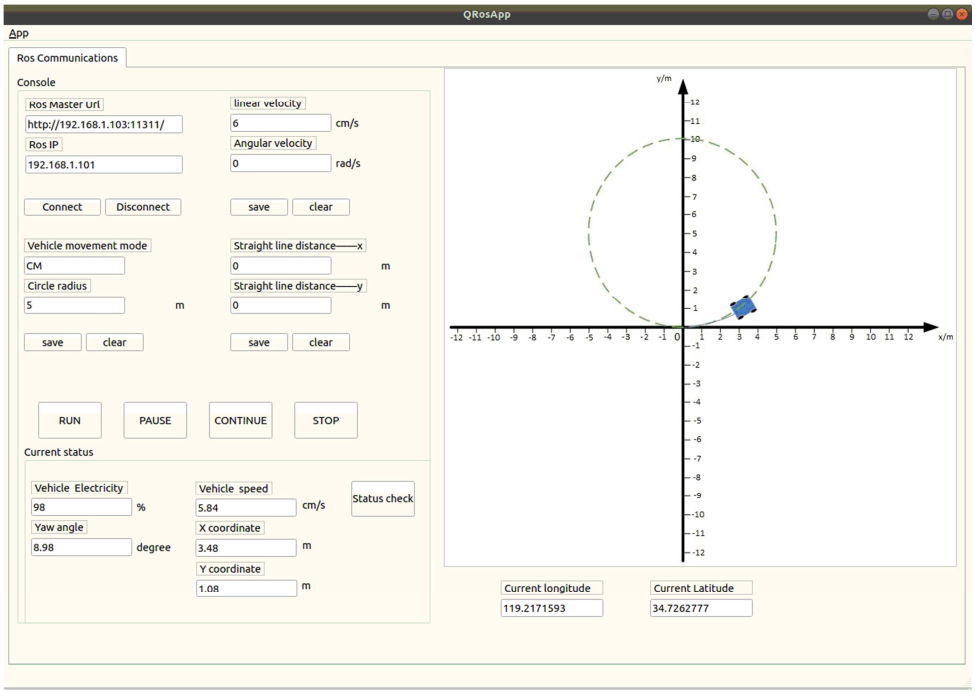

Figure 7. *QT-based development of the upper computer.*

Two groups of experiment are deployed. In Group a, the omnidirectional mobile robot started from the origin of the navigation space and moved in a circle with a radius of 8 m at a speed of 4 cm/sec. The trajectories of the different sensors and algorithms were recorded in turn. Figure 8 shows the localization trajectory data for different sensors and algorithms in the experiment of Group a. Figure 9 shows the local details of the positioning trajectories of the various algorithms and sensors in the experiment of Group a (at the start of the movement).

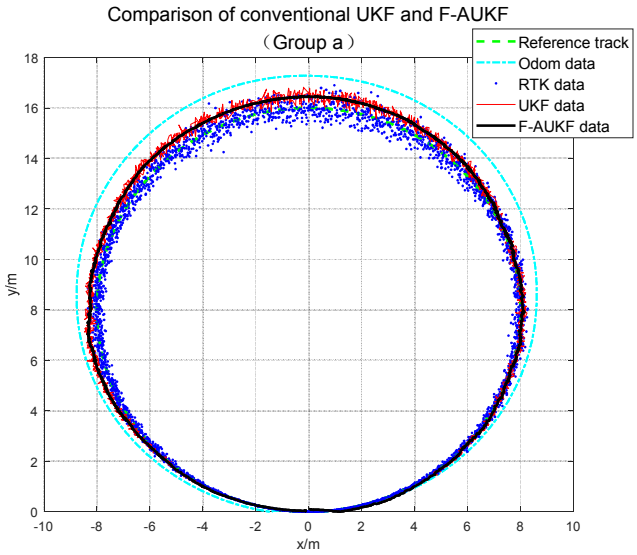

Figure 8. *Comparison of conventional UKF and F-AUKF (Group a).*

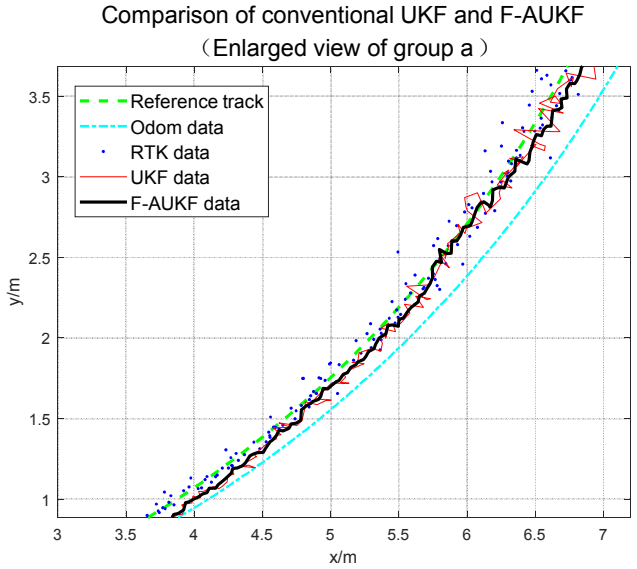

Figure 9. *Comparison of conventional UKF and F-AUKF (Enlarged view of Group a).*

In Group b, the robot moves on a circle with a radius of 5m at a speed of 6cm/sec. The data are recorded in same manner as for the experiments in Group a. Figure 10 illustrates the localization trajectory data for different sensors and algorithms in the experiment of Group b. Figure 11 shows the local details of the localization trajectories of the various algorithms and sensors in the experiment of Group a (moving for a period of time).

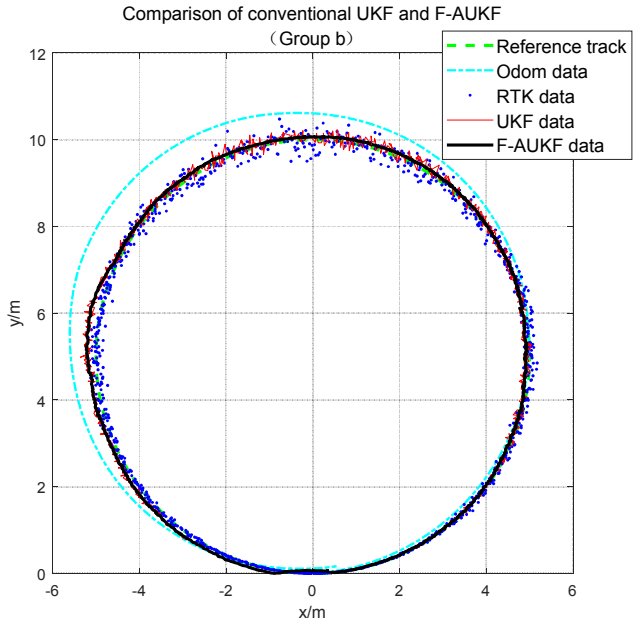

Figure 10. *Comparison of conventional UKF and F-AUKF (Group b).*

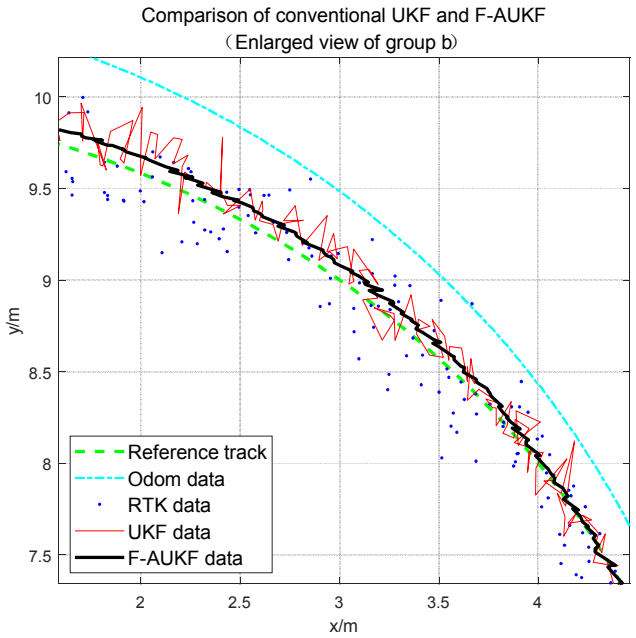

Figure 11. *Comparison of conventional UKF and F-AUKF (Enlarged view of Group b).*

All experiments show that the odometer data drift obviously from the reference trajectory due to the accumulated errors; the RTK trajectory curve fluctuates significantly around the reference trajectory, indicating that the RTK positioning is affected by the complex industrial environment and there is significant noise, but there is no cumulative error and the trajectory does not drift; the traditional UKF data are closer to the real trajectory than that of the odometer and RTK, that

sensor-fusion presents higher positioning accuracy. However, the filtering effect in the second half of the trajectory in Figure 9 obviously has some divergence, and the divergence effect in the whole part of Figure 11 is more obvious, which indicates that the positioning accuracy is not sustainable. The positioning trajectory filtered by the F-AUKF algorithm is closer to the reference trajectory than the positioning trajectory obtained by other positioning methods. In addition, the stability after a period of time is also significantly better than that of the traditional UKF algorithm.

To reveal the accuracy of the different positioning methods intuitively, the standard deviation formula is used to calculate the accuracy of several positioning methods:

$$\mu = \sqrt{\frac{1}{n}\sum_{i=0}^{n}(x_i - x_0)^2} \text{ or } \mu = \sqrt{\frac{1}{n}\sum_{i=0}^{n}(y_i - y_0)^2} \quad (13)$$

where μ represents the positioning accuracy in meter. x_i and y_i are the coordinates of x-direction or y-direction measured under different positioning methods. x_0 and y_0 are the coordinates of the x-direction or y-direction of the reference trajectory at the same moment, respectively.

The accuracy of different positioning methods is shown in Table 1:

Table 1. *Comparison of standard deviations of different positioning methods. unit: m.*

Group	Accuracy μ of different positioning methods	x-direction	y-direction
Group a	Odometry	1.2189	1.0878
	RTK	0.5928	0.4935
	Traditional UKF	0.2858	0.2026
	F-AUKF	0.0955	0.0356
Group b	Odometry	0.8095	0.6742
	RTK	0.5757	0.6259
	Traditional UKF	0.2624	0.3325
	F-AUKF	0.1316	0.1062

5. Conclusion

A mobile robot positioning algorithm is proposed in this paper. The algorithm applies sensor fusion and modified adaptive UKF with a forgetting factor. Experiments are design in several groups to validate the applicability of the algorithm. The experimental results show that the F-AUKF algorithm finally obtains a positioning accuracy that is about ten times better than the single odometer positioning accuracy, about six times better than the single RTK positioning accuracy and about three times better than the traditional UKF algorithm in a complex industrial environment, effectively improves the problem of filtering effect scattering after a long period of operation, and has better stability.

References

[1] Jun, F. U., X. U. Da, and F. U. Yang. "Application of an adaptive UKF in UWB indoor positioning." Bulletin of Surveying and Mapping (2019). doi: 10.1109/CAC48633.2019.8996692.

[2] J. Sun, L. Tao, Z. Niu and B. Zhu, "An Improved Adaptive Unscented Kalman Filter With Application in the Deeply Integrated BDS/INS Navigation System," in IEEE Access, vol. 8, pp. 95321-95332, 2020. doi: 10.1109/ ACCESS.2020.299574.

[3] Yuan, J., Luo, H., Yu, L., Luo, M., & Shi, J. J.. (2020). Performance assessment of single frequency gnss rtk/mems-imu combined positioning. Journal of Physics Conference Series, 1544, 012166. doi: 10.1088/1742-6596/1544/1/012166.

[4] Yuan, D., Zhang, J., Wang, J., Cui, X., Liu, F., & Zhang, Y.. (2021). Robustly adaptive ekf pdr/uwb integrated navigation based on additional heading constraint. Sensors (Basel, Switzerland), 21 (13). doi: 10.3390/s21134390.

[5] Zhan, M., & Xi, Z. H.. (2020). Indoor location method of wifi / pdr fusion based on extended kalman filter fusion. Journal of Physics Conference Series, 1601, 042004. doi: 10.1088/1742-6596/1601/4/042004.

[6] Hu, F., & Wu, G.. (2020). Distributed error correction of ekf algorithm in multi-sensor fusion localization model. IEEE Access, PP (99), 1-1. doi: 10.1109/ACCESS.2020.2995170.

[7] El Din, M. S., Hussein, A. A., & Abdel-Hafez, M. F.. (2018). Improved battery soc estimation accuracy using a modified ukf with an adaptive cell model under real ev operating conditions. IEEE Transactions on Transportation Electrification, 1-1. doi: 10.1109/TTE.2018.2802043.

[8] J. Feng, F. Cai, J. Yang, S. Wang and K. Huang, "An Adaptive State of Charge Estimation Method of Lithium-ion Battery Based on Residual Constraint Fading Factor Unscented Kalman Filter," in IEEE Access, vol. 10, pp. 44549-44563, 2022. doi: 10.1109/ACCESS.2022.3170093.

[9] Zhuang, J. H. (2015). Research on GPS precise positioning system based on real-time dynamic differencing of carrier phase. Unpublished master's thesis, Harbin University of Science and Technology, Harbin.

[10] Moore, T.. (2019). Understanding gps/gnss: principles and applications, third edition. The Aeronautical journal (123-Aug. TN. 1266).

[11] Yang Cheng, Shi Wenzhong, Chen Wu. (2016). Comparison of Unscented and Extended Kalman Filters with Application in Vehicle Navigation. Journal of Navigation, 70 (2): 411-431. doi: 10.1017/S0373463316000655.

[12] Madhukar, P. S., & Prasad, L. B.. (2020). State Estimation using Extended Kalman Filter and Unscented Kalman Filter. 2020 International Conference on Emerging Trends in Communication, Control and Computing (ICONC3). doi: 10.1109/ICONC345789.2020.9117536.

[13] Kolakowski, M.. (2020). Comparison of Extended and Unscented Kalman Filters Performance in a Hybrid BLE-UWB Localization System. 2020 23rd International Microwave and Radar Conference (MIKON). doi: 10.23919/MIKON48703.2020.9253854.

[14] Sever, M., & Hajiyev, C.. (2021). Gnss signal processing with ekf and ukf for stationary user position estimation. WSEAS Transactions on Signal Processing (17-), 17. doi: 10.37394/232014.2021.17.10.

[15] Allotta, B., Chisci, L., Costanzi, R., Fanelli, F., Fantacci, C., & Meli, E., et al. (2015). A comparison between EKF-based and UKF-based navigation algorithms for AUVs localization. Oceans (pp. 1-5). IEEE. doi: 10.1109/OCEANS-Genova.2015.7271681.